SEPARATION OF LAYOVER IN SYNTHETIC APERTURE INTERFEROMETRY

Stig A. V. Synnes Norwegian Defence Research Establishment (FFI), Kjeller, Norway
Marc Geilhufe Norwegian Defence Research Establishment (FFI), Kjeller, Norway

1 INTRODUCTION

Synthetic aperture sonar (SAS)[1] has become a well-established technique for underwater acoustical imaging of the seafloor. Recent 3D renderings of interferometric SAS recordings on ship wrecks have illustrated the huge potential of interferometric systems also for mapping of complex structures[2]. 3D renderings of ship wrecks, as the one we present in Fig. 1, have revealed a large number of valuable interferometric height measurements both on near vertical surfaces, and even in layover regions where multiple surfaces are overlaid in the SAS images. In some of the layover regions, the interferometric phase measurements appear to interchange between the different surfaces. In this paper we explore whether nearby measurements from interchanging surfaces can be extended to provide simultaneous measurements on multiple surfaces. We investigate the fundamentals of interferometry in layover regions, and also touch upon the potential bias that surfaces in a layover region might impose on the estimation of each other.

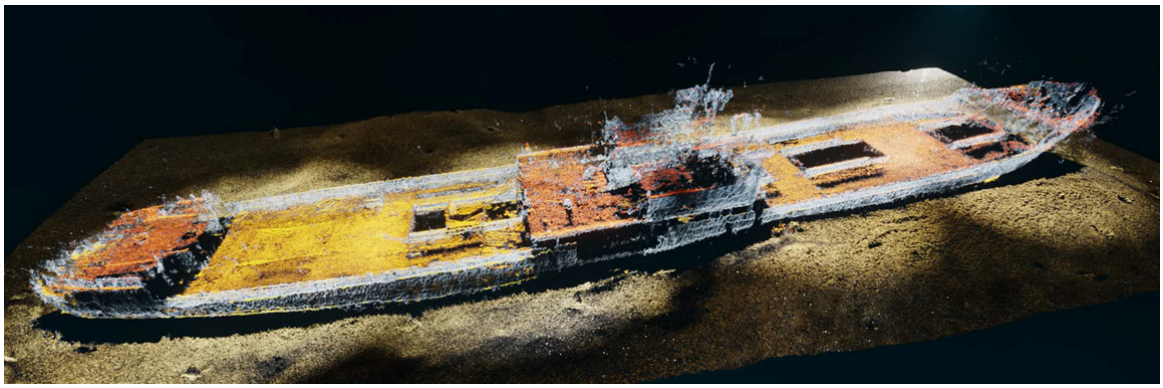

Figure 1: *3D rendering of wreck 18 from the Skagerrak munitions dump site, illustrating the value of height measurements on elevated structures, and the potential of resolving multiple surfaces in layover regions[2].*

The effect of layover is typically observed on man-made objects, as illustrated in Fig. 2, but it can also occur on steep terrain. The established method of obtaining height estimation from interferometric measurements exploits a cross-correlation based search over candidate lags[3]. However, such a search can resolve multiple heights in a layover region only with large separations between surfaces, where the absolute phase shift exceeds the range resolution[4]. We seek to advance on these limitations to resolve layover from shifts that are smaller than the range resolution. Furthermore, we aim to get the most out of a single-pass recording with an interferometric system, and therefore exclude multi-pass and multi-array techniques of both SAS[5] and SAR[6] in this study.

We establish a theoretical foundation of our work, by building a statistical model of interferometric samples drawn from a layover region, assuming speckle image statistics on each surface. Using this model, we explore different methods for estimation of the interferometric phase related to each surface in a layover region. We expand on our previous findings[7] on the topic, and suggest a robust

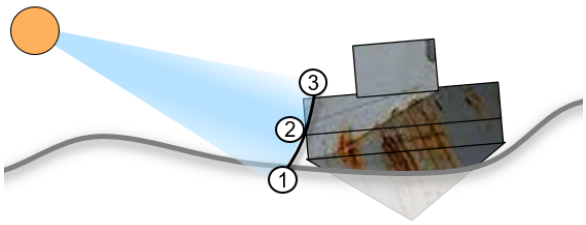

Figure 2: *Illustration of layover involving three surfaces observed at the same range: 1) Seafloor, 2) Hull, and 3) Deck.*

.

method for separation of layover. The performance of our suggested method is validated on simulated data. We find that the method efficiently separates overlaid surfaces of similar echo strength, but that its performance rapidly drops when surfaces of different echo strength are involved. Finally, we demonstrate the performance of our method on single-pass interferometric SAS data from a simple simulated scene and from real SAS data of a complex ship wreck.

2 MODELLING OF LAYOVER

In this section we build a statistical model of interferometric samples from surfaces with speckle image statistics, covering both one surface and layover involving multiple surfaces at the same range.

2.1 Speckle image statistics

Acoustical measurements of the seafloor are known to show speckle modulations on top of the seafloor texture and backscattering strength. These speckle variations originate from the superimposed backscattering of randomly distributed scatterers within each resolution cell[8]. The statistics of speckle is well known, and will be adopted for our study where we approximate that neighbour samples are drawn from the same speckle distribution. In the presence of layover, the contributions from each of the overlaid speckle surfaces are added together into a sample.

We first summarize some of the statistical properties of speckle[8]: Samples drawn from a speckle distribution, s, belong to a circularly symmetric complex Gaussian distribution. The real and imaginary components of a speckle distribution thus form independent random variables drawn from the same zero-mean normal distribution: $Re\{a\}$ and $Im\{a\} \sim N(\mu = 0, \sigma^2)$. The normal distribution, $N(\mu, \sigma^2)$, has the probability density function (PDF)

$$f(x; \mu, \sigma^2) = \frac{1}{\sigma\sqrt{2\pi}} e^{-\frac{1}{2}\left(\frac{x-\mu}{\sigma}\right)^2}, \tag{1}$$

with mean μ and variance σ^2. Samples drawn from a speckle distribution are uniformly distributed in phase and Rayleigh-distributed in amplitude: $|a| \sim \text{Rayleigh}(\sigma)$. The PDF of a Rayleigh distribution is

$$f(x; \sigma) = \frac{x}{\sigma^2} e^{-\frac{x^2}{2\sigma^2}}, \; x \geq 0, \tag{2}$$

with mean value of $\sigma\sqrt{\pi/2}$. The resulting intensity, $|a|^2$, of the speckle distribution samples is exponentially distributed, $|a|^2 \sim \text{Exp}(\lambda)$, with $\lambda = 1/(2\sigma^2)$, or $\sigma = 1/\sqrt{2\lambda}$. The PDF of an exponential distribution is

$$f(x; \lambda) = \lambda e^{-\lambda x}, \; x \geq 0, \tag{3}$$

with mean value $1/\lambda$. The mean of the exponential distribution is related to the mean of the Rayleigh distribution, which in turn is closely related to the acoustical backscattering strength.

2.2 Interferometry on layover

We model the data recorded at the two vertically displaced receivers, $s_1(t)$ and $s_2(t)$ as a weighted sum of three normalized time series $a(t)$, $b(t)$ and $c(t)$ at receiver 1, and as a shifted combination at receiver 2. In addition, we model different realizations of white Gaussian noise, $n_i(t)$, added at the two receivers:

$$\begin{aligned} s_1(t) &= Aa(t) + Bb(t) + Cc(t) + Nn_1(t) \\ s_2(t) &= Aa(t-\tau_a) + Bb(t-\tau_b) + Cc(t-\tau_c) + Nn_2(t) \end{aligned} \tag{4}$$

where τ_a, τ_b and τ_c express the different shifts (or delays convertible to depression angles) related to each surface[3].

The interferometric collection geometry is chosen such that corresponding pixels from an interferometric pair of SAS-images will contain the same realization of the speckle statistics after co-registration. We assume that the signals are co-registered to within a fraction of the resolution cell, through delaying by $\tau(t)$. Such simultaneous co-registration of all layover surfaces implies that we are treating layover on relatively small objects.

White Gaussian noise will have uniformly distributed phase and Rayleigh-distributed amplitude, just as speckle. The difference is that the noise takes different realizations on the two banks, in contrast to the speckle return which is identical on both banks after co-registration. We now compute the interferogram $\hat{\Gamma}$ between the two signals, s_1 and s_2,

$$\hat{\Gamma}(t,\tau) = \langle s_1^*(t) s_2(t-\tau) \rangle \,. \tag{5}$$

Inserting (4) into (5) gives

$$\begin{aligned} \hat{\Gamma}(\tau,\tau_a,\tau_b,\tau_c) &= A^2 a^*(\tau)a(\tau-\tau_a) + B^2 b^*(\tau)b(\tau-\tau_b) + ... \\ &\quad C^2 c^*(\tau)c(\tau-\tau_c) + N^2 n_1^*(\tau)n_2(\tau) \qquad (6) \\ &\approx A^2 e^{i\omega_c(\tau-\tau_a)} + B^2 e^{i\omega_c(\tau-\tau_b)} + C^2 e^{i\omega_c(\tau-\tau_c)} + N^2 n_1^*(\tau)n_2(\tau) \qquad (7) \end{aligned}$$

where the approximation assumes that all signals are simultaneously co-registered to where only the phase difference remains. The interferometric phase difference (modulo 2π) is available through $\hat{\psi} = \angle\hat{\Gamma}(f_c)$. Without layover, only one surface will contribute (i.e. $B = 0$ and $C = 0$), while the impact of noise reduces with the number of samples. Therefore, the established estimator of the interferometric phase for one surface, A, is to estimate the phase of the ensemble average[3].

With layover, the ensemble average only provides the combined effect from all surfaces. In order to obtain an estimate of the contribution from each surface, we suggest to establish the PDF of the interferogram for the layover region and to explore methods of extracting the interferometric phase corresponding to each surface based on this combined PDF.

2.3 Complex PDF for interferogram on layover

We now establish the probability density distribution (PDF) of the combined interferogram for a layover region. We exploit that the PDF for a sum of contributions is given by the convolution of their individual PDFs. Also, in the vicinity of the correct time delay, $\tau \approx \tau_i$, the contribution from each surface to the interferogram is proportional to its intensity. Therefore, while the phase follows from the scene elevation, the magnitude follows the exponential distribution of (3) with $\lambda = 1/(2\sigma^2)$. The independent realizations of noise on the two banks will upon evaluating the interferogram express the difference between independent samples with speckle statistics. The noise contribution to the interferogram is thus characterised by random phase and magnitude drawn from a Rayleigh distribution (2), with standard deviation $\sigma_{Rayl} = \sigma\sqrt{2}$, where σ is the standard deviation of the related normal distribution. We can now express the PDF of the interferogram as

$$f(x;\Gamma) = f(x_a;A) \otimes f(x_b;B) \otimes f(x_c;C) \otimes f(x_n,\tau_n;N) \tag{8}$$

with

$$f(x_a; A) = e^{i\omega(\tau-\tau_a)} \frac{1}{2A^2} e^{-\frac{x_a}{2A^2}} \quad (9)$$

$$f(x_n, \tau_n; N) = \frac{1}{2\pi} e^{i\omega\tau_n} \frac{x_n}{2\sigma^2} e^{-\frac{x_n^2}{4\sigma^2}} \quad (10)$$

where $x_i > 0$ for $i \in \{a, b, c, n\}$ and $\tau_n \in [0, 2\pi\rangle$. We observe that the expectation value for each surface contribution is $1/\lambda = 2\sigma^2$, which matches also the expectation value for the single layer case. For noise the expectation value for the ensemble is zero, while the expected magnitude of each sample is $\sigma\sqrt{\pi/2}$.

We show an example PDF for layover in Fig. 3, with source levels 0 dB, -5 dB and -10 dB, corresponding interferometric phases of 0°, 120° and -120°, and white Gaussian noise of -20 dB. We also illustrate an ensemble of 100 samples drawn from the distribution, together with their individual contributions from each of the three sources and from noise.

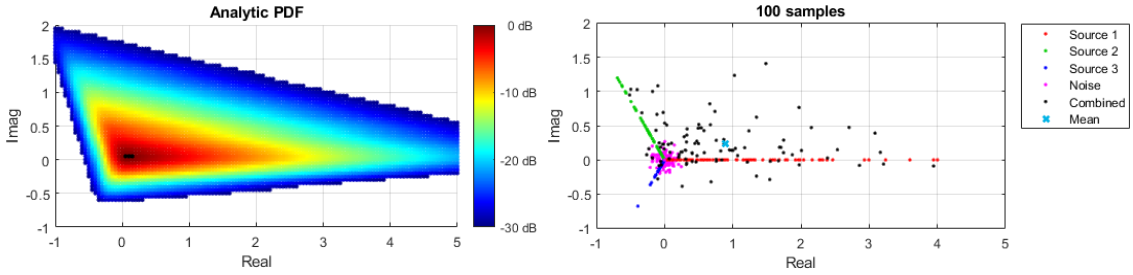

Figure 3: *Effect from layover of three surfaces with source levels of 0 dB, -5 dB and -10 dB, corresponding interferometric phases of 0°, 120° and -120°, and white Gaussian noise of -20 dB. Left: The analytic PDF obtained from (8). Right: One realization of 100 samples drawn from the PDF (black), the individual contributions (red, green and blue) and contribution from noise (magenta). We also indicate the ensemble mean (light blue).*

3 SEPARATION OF LAYOVER

We now investigate how to separate sources from a layover region, by exploiting the knowledge on their combined PDF to estimate the parameters of the individual sources.

Both the maximum likelihood method and the least squares have been explored for estimating the parameters of a mixture of exponential and Rayleigh distributions[9]. However, for our case with multiple exponential sources and individual phases, we have been unable to find any such solution. Since the published solutions for the simpler case are rather complex, we have not attempted to expand these solutions to our case.

A maximum likelihood estimator would be derived based on the goodness of fit on the log likelihood function. We recognize that using a metric based on the goodness of fit might be attempted for hypothesis testing in a search algorithm. We found a candidate in the Kolmogorov-Smirnov test extended to 2D distributions[10]. In an initial work, the performance of such a search showed some potential, but was both time consuming and sensitive to the start point[7].

From Fig. 3, we observe that the logarithm of the 2D PDF form close to planar faces, and we deduce that information on the originating sources might be readily obtained from the slope of these faces. Kernel smoothing is a well established method for estimating both the empirical CDF and the PDF from finite data samples. However, with our exponential distribution of the signal strength, the data points containing the most valuable information are sparse. We also have the additional disadvantage that we need to estimate a 2D PDF. Furthermore, the 2D PDF is not our end goal, but rather a means to estimate its underlaying parameters, perhaps through the slope of its faces. For

these reasons, direct 2D kernel smoothing does not promise a simple or directly applicable solution to our problem.

From Fig. 3, we note that the shape of the 2D PDF could be represented by any of its contour lines. The boundary (e.g. the convex hull) of the samples provides such a contour, but is sensitive to outliers as only a few extreme samples from the ensemble are used.

We suggest a new method that combines the simplicity of the boundary method with the robustness of kernel smoothing. We propose to apply kernel smoothing on the interferometric angle of the samples, and to use the intensity of the interferometric samples as kernel weights. We thereby incorporate all data samples into the estimate, and find that the method is less sensitive to outliers than the boundary method. We smoothen the output of the estimator, before we interpret the phases corresponding to prominent peaks as the interferometric phase corresponding to different surfaces of the layover problem. In Fig. 4 we illustrate this method, applied to the data samples of Fig. 3.

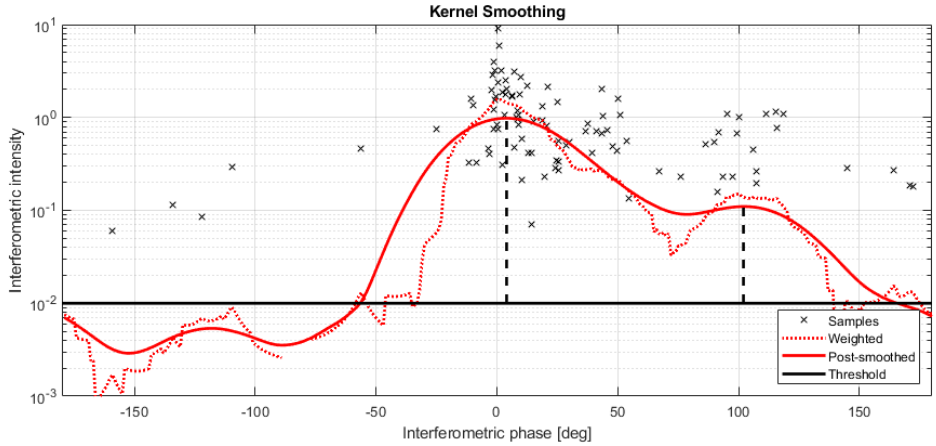

Figure 4: *Illustration of our suggested method for resolving layover based on kernel smoothing, here applied on the 100 data samples of Fig. 3 with true interferometric phases at 0°, 120° and -120° and corresponding source levels of 0 dB, -5 dB and -10 dB. The interferometric samples (x) are kernel smoothed on the phase axis, employing their intensity as weights, to give a raw output (red dotted line). This output is post-smoothed (red line), before local peaks are detected and adopted as phase estimates, here found at 2° and 104° (black dashed lines). Peaks below the threshold (solid black line) are discarded in order to suppress false detections.*

4 RESULTS AND DISCUSSION

We apply our suggested method for separation of layover on ensembles of simulated samples, in order to quantify its performance. We have not yet derived the quality metric needed for optimizing a search over multiple candidate 2π-wraps, but attempt to illustrate the potential of our method by running it on both a simulated SAS and one real SAS dataset.

4.1 Simulated ensemble of samples

We now test our method for separation of layover and compare its performance to that of classical estimation of interferometric phase of a single surface. We draw an ensemble of 100 interferometric samples from the mixture of three sources with individual interferometric phase angles of 0°, 120° and -120° and different echo strengths. We apply both our suggested method and the classical method of interferometric phase estimation (using the sample mean). We repeat the process for 1000 ensembles to allow for computation of some statistical performance metrics. We run this experiment with tree different combinations of source strengths; three sources of equal strength, three sources with falling strength in steps of -5 dB, and finally three sources with falling strength in steps of -10 dB.

a)

Source Levels: 0 dB, 0 dB, 0 dB

	Classical	*Layover Surface 1*	*Layover Surface 2*	*Layover Surface 3*
Retrieval rate	(100%)	100%	95%	94%
Angle error STD	(104°)	6°	6°	6°
Angle error med.	(92°)	4°	4°	3°

b)

Source Levels: 0 dB, -5 dB, -10 dB

	Classical	*Layover Surface 1*	*Layover Surface 2*	*Layover Surface 3*
Retrieval rate	100%	100%	46%	0%
Angle error STD	3°	1°	5°	–
Angle error med.	13°	5°	11°	–

c)

Source Levels: 0 dB, -10 dB, -20 dB

	Classical	*Layover Surface 1*	*Layover Surface 2*	*Layover Surface 3*
Retrieval rate	100%	100%	0%	0%
Angle error STD	1°	1°	–	–
Angle error med.	5°	3°	–	–

Table 1: *Performance values for estimation of interferometric phase angles on a layover region with three sources at 0°, 120° and -120° and different combinations of source levels, shown in sub-tables a, b and c. One realization from sub-table b has been illustrated in Fig. 3 and Fig. 4.*

We summarize the results in Table 1. From Table 1a, we observe that with three sources of equal source strength, our suggested method retrieves good estimates of the interferometric phase for all the three sources in 94% of the sample ensembles. While the classical approach only obtains a random phase, the three phase estimates of our new method have no significant added bias, though some increased standard deviation.

From Table 1a and Table 1b we observe that with different strength of the three sources, the success rate of our method rapidly decreases. The phase of a source 5 dB weaker than the strongest one is only retrieved in 46% of the sample ensembles, while the phase of a 10 dB weaker source than the strongest one is never retrieved. From the illustrations of Fig. 3, we recognize that it may be difficult to recognize the contribution to the 2D PDF from a source of -10 dB, though it could be possible at least occasionally and when the noise is not too strong. We therefore recognize that the -5 dB limit probably does not constitute a fundamental limit.

While Table 1a, Table 1b and Table 1c were prepared using ensembles of 100 samples, changing the number of samples primarily affects the standard deviation and the median of the estimates. With ensembles of 10, 30, 100, 300 or 1000 samples, the results for three sources of equal strength (as with Table 1a) change to respectively standard deviations of 31°, 16°, 6°, 3° and 2° and medians of 11°, 6°, 4°, 2° and 1° for all three sources. The retrieval rate remains near unchanged.

4.2 Simulated SAS data

We have simulated a pair of images from an interferometric SAS system, corresponding that of the Kongsberg HISAS SAS on an HUGIN AUV[1]. The scene shows a box of length, depth and height of 5m x 5m x 2m, observed at 30 m range from 10 m altitude. We have applied our suggested method for separation of layover on a 9x9 pixel sliding window on the resulting interferogram, and present the results in Fig. 5. We observe that layer 1, corresponding to the surface with strongest intensity, is confusingly similar to a classical interferogram. The contents of layers 2 and 3 show that the algorithm has found multiple solutions within the sliding window on the sides of the box, where samples from two different elevations are included, and on the layover region in front of the box. We have not yet evaluated the quality of the phase estimates, but correctly localizing the areas with multiple solutions and resembling the interferogram in areas with a single solution is a promising start.

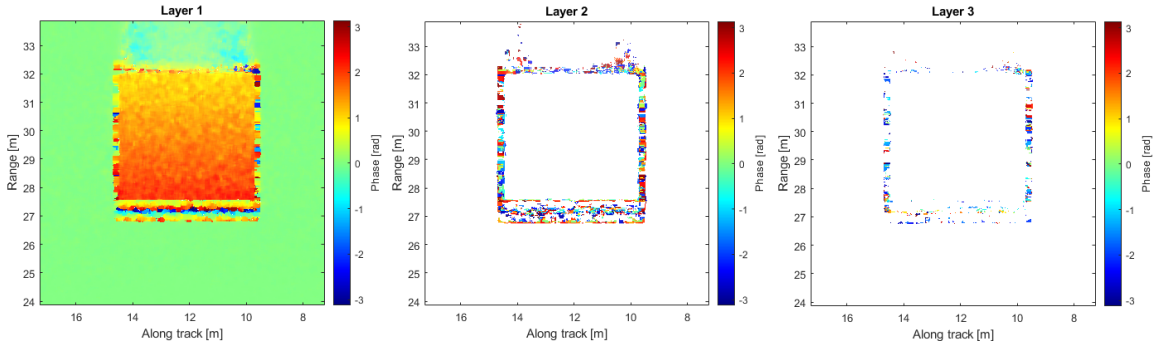

Figure 5: *Estimated phases for three layers with our suggested method for layover separation. Layer 1 closely resembles the solution of a classical sliding window interferogram, while layers 2 and 3 indicate areas with multiple surfaces within the 9x9 pixel window used.*

4.3 Recorded SAS data

In order to obtain altitude measurements from estimates of the interferometric phase on complex targets, we would have to first resolve the absolute phase from a search over multiple candidate lags[3]. As we have not yet derived the quality metric needed for optimizing such a search, we are restricted to present the wrapped phase estimates.

In Fig. 6 we present a SAS intensity image showing the aft section of a wreck on the seafloor, recorded with the Kongsberg HISAS interferometric SAS on the Hugin AUV. We have applied our suggested method for separation of layover on a 9x9 pixel sliding window on the interferogram, and also present three resulting layers of estimates. Also here, we observe that layer 1, strongly resembles the result of a classical interferogram. Layer 2, in particular, indicates areas with multiple solutions within the sliding window. Much of the shadow zone is also indicated in layer 2, but this area could be masked by considering the image intensity. The method thus looks promising for localizing areas with multiple surfaces. In addition, large areas with similar phase in layer 2 indicates that there is consistency also in the estimated phase values.

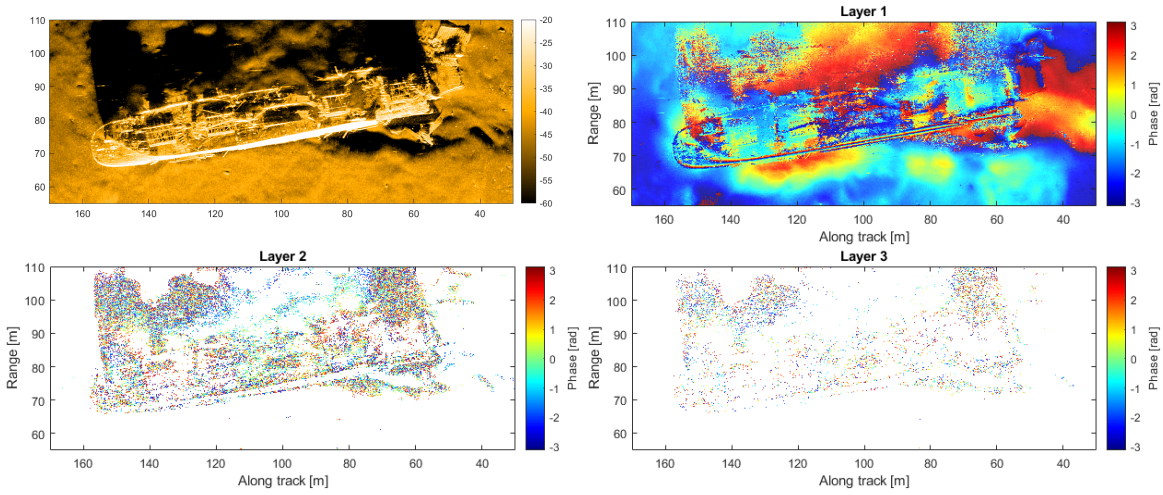

Figure 6: *Results on wreck 13 of the Skagerrak munitions dump site, showing an intensity image to the upper left, together with the estimated phases over three layers, using our suggested method for layover separation within a 9x9 pixel sliding window. Layer 1 closely resembles the solution of a classical sliding window interferogram, while layer 2, and to some extent layer 3, indicates areas with multiple surfaces with their interferometric phases.*

5 CONCLUSION

We have suggested a robust method for separation of layover on single-pass interferometric SAS data. The suggested method is based on kernel smoothing on the phase of the interferometric samples, while incorporating their intensity as weights. Furthermore, we established a statistical model for interferometric samples from a layover region, and evaluated the performance of our method on modelled interferometric data. We found that our suggested method could separate surfaces of similar echo strength in a layover region, but that its performance rapidly drops for surfaces with echo strength lower than 5 dB below that of the other surfaces. We finally showed results from applying our new method both on a simple simulated scene and on recorded SAS data on a complex ship wreck. We demonstrated correctly locating regions with layover and indicated consistency over the phase estimates.

6 ACKNOWLEDGMENTS

The authors would like to thank Roy E. Hansen, Torstein O. Sæbø and Ole J. Lorentzen at FFI for fruitful discussions and inputs during the preparation of this paper. The authors thank FFI's HUGIN-HUS operator group for collecting the data used in this study. This work was funded by the Norwegian Defence and Kongsberg Discovery, through a long-term collaboration on the development of SAS for the Royal Norwegian Navy.

7 REFERENCES

1. R. E. Hansen, *Introduction to Synthetic Aperture Sonar*. InTech, 2011, DOI:10.5772/23122.

2. O. J. Lorentzen, R. E. Hansen, T. O. Sæbø, S. A. V. Synnes, and M. Geilhufe, "3D rendering of shipwrecks with synthetic aperture sonar," June 2021, available online: https://www.youtube.com/watch?v=J7rNeKaivkg.

3. T. O. Sæbø, S. A. V. Synnes, and R. E. Hansen, "Wideband interferometry in synthetic aperture sonar," *Transactions on Geoscience and Remote Sensing*, vol. 51, no. 8, pp. 4450–4459, 2013.

4. O. J. Lorentzen, S. A. V. Synnes, R. E. Hansen, and T. O. Sæbø, "Investigating layover effects in cross-correlation based interferometry for synthetic aperture sonar," in *12th European Conference on Synthetic Aperture Radar (EUSAR)*, 2018.

5. M. P. Hayes, A. J. Hunter, P. J. Barclay, and P. T. Gough, "Estimating layover in broadband synthetic aperture sonar bathymetry," in *Ocean Europe*, 2005, pp. 1068–1073.

6. A. Pepe and F. Calo, "A review of interferometric synthetic aperture radar (InSAR) multi-track approaches for the retrieval of Earth's surface displacements," *Applied Sciences (Switzerland)*, vol. 7, no. 12, pp. 1–39, 2017.

7. S. A. V. Synnes, M. Geilhufe, R. E. Hansen, T. O. Sæbø, and O. J. Lorentzen, "Investigation of layover in interferometry (presentation only)," in *International Conference on Underwater Acoustics (ICUA), June 23 2022, Southampton*, 2022.

8. C. Oliver and S. Quegan, *Understanding Synthetic Aperture Radar Images, Chapter 4.3*, 1st ed. Artech house, Inc., 1998.

9. J. Hussain and A. Shareef, "Parameters estimation of new mixed Weibull Rayleigh and exponential distribution," in *Journal of Physics: Conference Series*, vol. 1879, no. 2, 2021.

10. G. Fasano and A. Franceschini, "A multidimensional version of the Kolmogorov-Smirnov test," *Mon Not R Astr Soc 225: 155-170*, 1897.